

# Optimal Low-Complexity Orthogonal Block Based Detection of OTFS for Low-Dispersion Channels

Wei Liu, *Senior Member, IEEE*, Yajie Ding, Chuan Li, Lajos Hanzo, *Life Fellow, IEEE*

**Abstract**—Orthogonal time frequency space (OTFS) modulation constitutes a promising technology for high-mobility scenarios. However, the detection of OTFS systems imposes substantial complexity. Hence, we propose a novel orthogonal block (OB) based detection scheme for significantly reducing the OTFS detection complexity without any performance loss with integer Doppler shifts. This is achieved by recognizing that the received signal can be partitioned into multiple parallel orthogonal blocks. Therefore, the detection of data symbols within an orthogonal block only depends on the signals received within this orthogonal block with reduced dimension. Explicitly, we propose a graph theory based orthogonal block identification algorithm, which models the relationship between the received signal and the original information symbols as a bipartite graph, where a depth first search (DFS) algorithm is invoked for partitioning the received signals into orthogonal blocks. For each orthogonal block, the existing detection algorithms can be used. Since the size of orthogonal blocks may be much lower than that of the original received signals, the detection complexity can be significantly reduced. For example, the complexity of the OB based MMSE detector is approximately a factor 4096 lower than that of the traditional MMSE detector for a channel having two paths.

## I. INTRODUCTION

High-mobility wireless communication scenarios exhibit high Doppler spread, for example for unmanned aerial vehicle (UAV) [1], airplanes [2], low-earth-orbit (LEO) satellites [3], and so on. Hence traditional OFDM schemes suffer from severe inter-carrier interference (ICI) [4]. Recently, an Orthogonal Time Frequency Space Modulation (OTFS) modulation technique has been proposed as a promising solution for high-mobility communication scenarios [5]–[7]. Explicitly, OTFS places data symbols in the delay-Doppler (DD) domain and converts the time-varying channel into an approximately time-invariant channel in the DD domain, so as to outperform the traditional OFDM in high-mobility scenarios [5].

Briefly, the detection is carried out jointly in the DD domain, which however imposes significant computational

burden upon using traditional detection schemes such as minimum mean squared error (MMSE) and maximum a posteriori (MAP) detectors. Hence, low-complexity OTFS detection algorithms have attracted intensive research interests. In [8], a Markov chain Monte Carlo (MCMC) sampling based detection algorithm was proposed. In [9] a message passing (MP) based detection algorithm was conceived, relying on the Gaussian approximation of the interference term for reducing the complexity of the algorithm. Furthermore, in [10] a variational Bayesian detector was designed, which outperforms the MP algorithm of [9]. Moreover, in [11], an improved approximate message passing (AMP) detection algorithm was conceived, which outperforms the traditional AMP algorithm. In [12], a multi-block unitary approximate message passing (UAMP) detection algorithm was designed by partitioning a large time-domain channel matrix into several sub-matrices. In [13], a maximal ratio combining receiver was proposed to blockwisely detect symbols. In [14], a low complexity iterative rake decision feedback equalizer was proposed. In [15], a hybrid detection algorithm was put forward by combining the MAP detector and parallel interference cancellation (PIC) detector. In [16], a cross-domain iterative detection algorithm was proposed by exchanging extrinsic information between the time domain and DD domain. Furthermore, in [17], low complexity MMSE and zero-forcing (ZF) detectors were proposed by exploiting the unique characteristics of the OTFS channel matrix for optimizing the traditional MMSE and ZF detectors.

The above solutions mainly focus on the performance vs. detection complexity trade-off without any dimension reduction, despite the fact that the classic sparse DD domain fading channel only introduces interferences to specific subsets of the received signals. Against this background, we propose a novel optimal low-complexity orthogonal block (OB)-based detection scheme capable of operating without any performance loss in the OTFS system with integer Doppler shifts. In Table I, we boldly and explicitly contrast our contributions to the state-of-the-art. Our main contributions are detailed as follows:

- We discover the inherent nature of orthogonal blocks in the OTFS system with integer Doppler shifts. Specifically, we demonstrate that the received signals can be approximately partitioned into several orthogonal blocks, each of which may be detected without any influence of the other blocks. In other words, the detection of data symbols contained in a specific orthogonal block only depends on the signals received within this orthogonal block. Hence, for each orthogonal block, any existing

W. Liu and Y. Ding are with State Key Labs of Integrated Service Networks, Xidian University, 710071, Xi'an, Shaanxi, P. R. China. Email:liuweixd@mail.xidian.edu.cn; yjding\_1@stu.xidian.edu.cn.

C. Li is with the School of Computer and Technology, Xian University of Posts and Telecommunications, Xian 710061, China. E-mail:lichuan@xupt.edu.cn.

L. Hanzo is with the School of Electronics and Computer Science, University of Southampton, SO17 1BJ Southampton, U.K. E-mail:{cx1g08,lh@ecs.soton.ac.uk.}

The financial support of National Natural Science Foundation of China under Grant (61871452) is gratefully acknowledged.

L. Hanzo would like to acknowledge the financial support of the Engineering and Physical Sciences Research Council projects EP/W016605/1 and EP/P003990/1 (COALESCE) as well as of the European Research Council's Advanced Fellow Grant QuantCom (Grant No. 789028).

TABLE I: Our Contributions Against the State-of-Art Detection Schemes

		Our OB Based Detection Algorithm	MAP	Traditional MMSE	MCMC [8]	MP [9]	AMP [11]	VB [10]	Low Complexity MMSE [17]	UAMP [12]
complexity	high		✓		✓					
	middle			✓						✓
	low	✓				✓	✓	✓	✓	
Optimality achievable		✓	✓							
Compatibility		✓								
Parallel processing		✓								
Dimension reduction		✓								

detection algorithm can be used. As an explicit benefit, our scheme is compatible with any existing detection scheme. Since each orthogonal block may have a much smaller size than the original OTFS block, the complexity is significantly reduced. Furthermore, our OB-based scheme supports parallel processing for multiple orthogonal blocks, which is suitable for practical implementation for large scale systems.

- We propose a graph theory based orthogonal block partitioning algorithm. Specifically, we model the relationship between the received signal and original symbols by a bipartite graph. Based on this bipartite graph model, the depth first search (DFS) algorithm is invoked for delineating the orthogonal blocks. Again, once the orthogonal blocks have been delineated, any existing detection algorithm can be invoked for each block.
- The number of orthogonal blocks depends on the number of paths in the channels. The lower the number of the paths, the more orthogonal blocks we have, which results in smaller size of blocks. Moreover, the smaller size of each block results in a reduced complexity detection algorithm. Hence, our OB based scheme is beneficial for low-dispersion channels, which are routinely encountered in the high-Doppler scenario. For example, the complexity of the OB based MMSE detector is approximately a factor 4096 lower than that of the traditional MMSE detector for a two-path channel.

Note that the philosophy of transforming a large-scale block into multiple parallel sub-blocks of smaller size, where existing detection algorithms may be invoked for each sub-block, is widely adopted in wireless communication. For example, in [18], a large-scale OFDM system was transformed into multiple reduced-size sub-blocks, where the maximum likelihood detector was harnessed for each sub-block at a reduced complexity. Another example is constituted by the multiuser MIMO downlink, where a block-digitalization algorithm was proposed for suppressing the multi-user interference, so that classic single-user detection algorithms can be invoked for each sub-block [19].

## II. SYSTEM MODEL

For the OTFS system, for the maximum delay  $\tau_{max}$  and maximum Doppler  $\nu_{max}$ , a total bandwidth of  $B = M\Delta f$  and time duration  $T_f = NT$  associated with  $\Delta f = 1/T$ , where  $\Delta f$  is the subcarrier spacing and  $T = 1/\Delta f$  is the symbol duration [10], are invoked

for transmitting  $NM$  data symbols under the constraints  $\tau_{max} < 1/\Delta f$  and  $\nu_{max} < 1/T$  [9]. The  $NM$  data symbols  $\{x[k, l], k = 0, \dots, N-1, l = 0, \dots, M-1\}$  are transmitted in the DD domain where  $x[k, l]$  is drawn from the constellation set  $\mathcal{A}$ .

Furthermore, the channel  $h(\tau, \nu)$  is composed of  $P$  propagation paths and can be expressed as [20]

$$h(\tau, \nu) = \sum_{i=1}^P h_i \delta(\tau - \tau_i) \delta(\nu - \nu_i), \quad (1)$$

where  $h_i, \tau_i$ , and  $\nu_i$  represent the channel gain, delay, and Doppler shift associated with the  $i^{th}$  path, and  $\delta(\cdot)$  denotes the Dirac delta function. Furthermore, the delay  $h_i$  and Doppler shift  $\nu_i$  and of the  $i^{th}$  path can be expressed as [20]

$$\tau_i = \frac{l_i}{M\Delta f}, \nu_i = \frac{k_i}{NT}, \quad (2)$$

where  $l_i$  and  $k_i$  represent the indices of delay and Doppler, respectively, while delay and Doppler taps  $l_\tau$  and  $k_\nu$  correspond to the largest delay  $\tau_{max}$  and largest Doppler  $\nu_{max}$  [9], respectively. In this paper, we only consider the case where  $l_i$  and  $k_i$  are integers.

Moreover, the signal  $y[k, l]$  received in the DD domain can be written as [20]

$$y[k, l] = \sum_{i=1}^P h'_i x[[k - k_i]_N, [l - l_i]_M] + z[k, l] \quad (3)$$

where we have  $h'_i = h_i e^{-j2\pi\nu_i\tau_i}$  [20].

## III. OPTIMAL LOW-COMPLEXITY ORTHOGONAL BLOCK DETECTOR

### A. Orthogonal Block Based Nature of OTFS

The matrix formulation of received signal in the DD domain can be expressed as [9]

$$\mathbf{y} = \mathbf{H}\mathbf{x} + \mathbf{n}, \quad (4)$$

where we have  $\mathbf{x}, \mathbf{y}, \mathbf{n} \in C^{MN \times 1}$ ,  $\mathbf{H} \in C^{MN \times MN}$ . Let us denote the  $(k + Nl)$ -th element of  $\mathbf{x}$  by

$$x_{k+Nl} = x[k, l] \quad (5)$$

and the  $(k + Nl)$ -th element of  $\mathbf{y}$  as

$$y_{k+Nl} = y[k, l], \quad (6)$$

where the elements in  $\mathbf{H}$  are placed according to the relationship between  $\{x_{k+Nl}\}$  and  $\{y_{k+Nl}\}$ .

$$\begin{bmatrix} y_0 \\ y_1 \\ y_2 \\ y_3 \\ y_4 \\ y_5 \\ y_6 \\ y_7 \\ y_8 \end{bmatrix} = \begin{bmatrix} h'_1 & 0 & 0 & 0 & 0 & 0 & 0 & 0 & h'_2 \\ 0 & h'_1 & 0 & 0 & 0 & 0 & h'_2 & 0 & 0 \\ 0 & 0 & h'_1 & 0 & 0 & 0 & 0 & h'_2 & 0 \\ 0 & 0 & h'_2 & h'_1 & 0 & 0 & 0 & 0 & 0 \\ h'_2 & 0 & 0 & 0 & h'_1 & 0 & 0 & 0 & 0 \\ 0 & h'_2 & 0 & 0 & 0 & h'_1 & 0 & 0 & 0 \\ 0 & 0 & 0 & 0 & 0 & h'_2 & h'_1 & 0 & 0 \\ 0 & 0 & 0 & h'_2 & 0 & 0 & 0 & h'_1 & 0 \\ 0 & 0 & 0 & 0 & h'_2 & 0 & 0 & 0 & h'_1 \end{bmatrix} \begin{bmatrix} x_0 \\ x_1 \\ x_2 \\ x_3 \\ x_4 \\ x_5 \\ x_6 \\ x_7 \\ x_8 \end{bmatrix}. \quad (7)$$

$$\begin{bmatrix} y_0 \\ y_4 \\ y_8 \\ y_2 \\ y_3 \\ y_7 \\ y_1 \\ y_5 \\ y_6 \end{bmatrix} = \begin{bmatrix} h'_1 & 0 & h'_2 & 0 & 0 & 0 & 0 & 0 & 0 \\ h'_2 & h'_1 & 0 & 0 & 0 & 0 & 0 & 0 & 0 \\ 0 & h'_2 & h'_1 & 0 & 0 & 0 & 0 & 0 & 0 \\ 0 & 0 & 0 & h'_1 & 0 & h'_2 & 0 & 0 & 0 \\ 0 & 0 & 0 & h'_2 & h'_1 & 0 & 0 & 0 & 0 \\ 0 & 0 & 0 & 0 & h'_2 & h'_1 & 0 & 0 & 0 \\ 0 & 0 & 0 & 0 & 0 & 0 & h'_1 & 0 & h'_2 \\ 0 & 0 & 0 & 0 & 0 & 0 & h'_2 & h'_1 & 0 \\ 0 & 0 & 0 & 0 & 0 & 0 & 0 & h'_2 & h'_1 \end{bmatrix} \begin{bmatrix} x_0 \\ x_4 \\ x_8 \\ x_2 \\ x_3 \\ x_7 \\ x_1 \\ x_5 \\ x_6 \end{bmatrix}. \quad (8)$$

For a 'toy' example, we assume that  $M = 3$  and  $N = 3$ . Furthermore, we assume that there are  $P = 2$  paths in the channel. Moreover, the corresponding delay and Doppler indices for the first path are  $l_1 = 0$  and  $k_1 = 0$ , respectively, while the corresponding delay and Doppler indices for the second path are  $l_2 = 1$  and  $k_2 = 1$ , respectively. Then, according to (4), we have (7), shown in the next page.

Interestingly, we can see that the received signal  $y_0$  is only composed of the pair of data symbols  $x_0$  and  $x_8$ , the received signal  $y_4$  is only composed of the pair of data symbols  $x_0$  and  $x_4$ , while the received signal  $y_8$  is only composed of pair of data symbols  $x_4$  and  $x_8$ . These three received signals can construct a block, which are only related to three data symbols  $x_0$ ,  $x_4$  and  $x_8$ . Similarly, the three received signals  $y_2$ ,  $y_3$  and  $y_7$  are only related to three data symbols  $x_2$ ,  $x_3$  and  $x_7$ , while the three received signals  $y_1$ ,  $y_5$  and  $y_6$  are only related to three data symbols  $x_1$ ,  $x_5$  and  $x_6$ .

Based on this observation, (7) can be equivalently expressed as (8), shown in the next page.

It can then be observed from the above formula that the received signals can be partitioned into three uncorrelated blocks associated with the corresponding data symbols of

$$\underbrace{\begin{bmatrix} y_0 \\ y_4 \\ y_8 \end{bmatrix}}_{\tilde{\mathbf{y}}_1} = \underbrace{\begin{bmatrix} h'_1 & 0 & h'_2 \\ h'_2 & h'_1 & 0 \\ 0 & h'_2 & h'_1 \end{bmatrix}}_{\tilde{\mathbf{H}}_1} \underbrace{\begin{bmatrix} x_0 \\ x_4 \\ x_8 \end{bmatrix}}_{\tilde{\mathbf{x}}_1} \quad (9)$$

$$\underbrace{\begin{bmatrix} y_2 \\ y_3 \\ y_7 \end{bmatrix}}_{\tilde{\mathbf{y}}_2} = \underbrace{\begin{bmatrix} h'_1 & 0 & h'_2 \\ h'_2 & h'_1 & 0 \\ 0 & h'_2 & h'_1 \end{bmatrix}}_{\tilde{\mathbf{H}}_2} \underbrace{\begin{bmatrix} x_2 \\ x_3 \\ x_7 \end{bmatrix}}_{\tilde{\mathbf{x}}_2} \quad (10)$$

$$\underbrace{\begin{bmatrix} y_1 \\ y_5 \\ y_6 \end{bmatrix}}_{\tilde{\mathbf{y}}_3} = \underbrace{\begin{bmatrix} h'_1 & 0 & h'_2 \\ h'_2 & h'_1 & 0 \\ 0 & h'_2 & h'_1 \end{bmatrix}}_{\tilde{\mathbf{H}}_3} \underbrace{\begin{bmatrix} x_1 \\ x_5 \\ x_6 \end{bmatrix}}_{\tilde{\mathbf{x}}_3}. \quad (11)$$

These three orthogonal blocks can be unified as

$$\tilde{\mathbf{y}}_i = \tilde{\mathbf{H}}_i \tilde{\mathbf{x}}_i + \tilde{\mathbf{n}}_i, 1 \leq i \leq 3, \quad (12)$$

where we have  $\tilde{\mathbf{x}}, \tilde{\mathbf{y}}, \tilde{\mathbf{n}} \in C^{3 \times 1}$ ,  $\tilde{\mathbf{H}}_i \in C^{3 \times 3}$ . For different orthogonal blocks, the received signals are composed of completely disjoint transmission symbol sets. Hence, the detection of the corresponding data symbols in the different blocks has no influence on each other. Consequently, we can separately detect the related data symbols by only using the received signal directly related to these orthogonal blocks.

Let us assume that there exist  $L$  orthogonal blocks. For the  $i$ th orthogonal blocks, we have

$$\tilde{\mathbf{y}}_i = \tilde{\mathbf{H}}_i \tilde{\mathbf{x}}_i + \tilde{\mathbf{n}}_i, 1 \leq i \leq L, \quad (13)$$

where  $\tilde{\mathbf{x}}, \tilde{\mathbf{y}}, \tilde{\mathbf{n}} \in C^{NM/L \times 1}$ ,  $\tilde{\mathbf{H}}_i \in C^{NM/L \times NM/L}$ . Any existing detection algorithm can be invoked for each orthogonal block. For a given OTFS block, the number of orthogonal blocks,  $L$ , depends both on the delay and Doppler shift, as we can see from the simulations.

### B. Graph Theory Based Orthogonal Block Identification Algorithm

As described above, we can design an orthogonal block identification algorithm, which can delineate the orthogonal blocks of OTFS and facilitate the subsequent data symbol detection.

The main idea is to partition the received signal vector of (4) into orthogonal blocks.

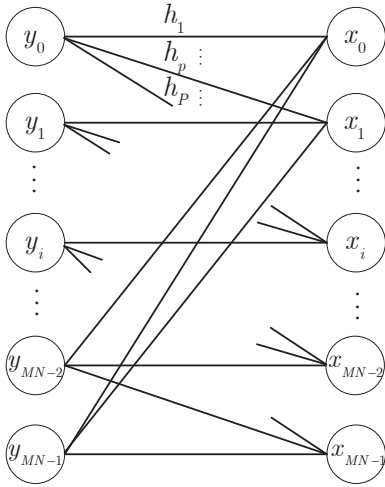


Fig. 1: Bipartite graph model of the relationship between the data symbols and received signals.

To this end, according to (4), we can use an undirected bipartite graph  $\mathcal{G} = (\mathcal{V}, \mathcal{E})$ , where  $\mathcal{V}$  and  $\mathcal{E}$  represent the sets of nodes and links in the bipartite graph  $\mathcal{G}$ , respectively, for modeling the relationship between the data symbol  $x_i$  and the received signal  $y_j$ , as shown in Fig. 1. Specifically, we have  $\mathcal{V} = \mathcal{V}_x \cup \mathcal{V}_y$ , where  $\mathcal{V}_x = \{x_i, i = 0, 1, \dots, NM - 1\}$  is the set of all data symbols, while  $\mathcal{V}_y = \{y_i, i = 0, 1, \dots, NM - 1\}$  is the set of all received signals. Furthermore, if we have  $h_{ij} \neq 0$ , there is a link  $e_{y_i, x_j}$  between node  $y_i$  and node  $x_j$ . Hence, we have  $\mathcal{E} = \{e_{y_i, x_j} | h_{ij} \neq 0\}$ . Moreover,  $\mathcal{V}_x$  and  $\mathcal{V}_y$  constitute a pair of disjoint node sets.

Based on the bipartite graph  $\mathcal{G}$ , we can use the classical DFS algorithm [21] to determine the relationship of nodes, hence also that of the orthogonal received signal blocks. Specifically, the algorithm consists of the following steps:

**Step 1:** Initialization. Label the vertices representing the received signals by odd numbers, while the vertices representing data symbols by even numbers. Furthermore, for each node  $i$ , construct its adjacent vertex set  $\mathcal{S}_i$ .

**Step 2:** Start the DFS algorithm [21] from the specific vertex having the smallest odd number. When the DFS algorithm stops, denote the set of vertices found by the DFS algorithm as

$$\mathcal{R} = \{j | \text{vertex}_j \text{ is found by the DFS algorithm}\}. \quad (14)$$

Naturally, the vertices associated with odd numbers in  $\mathcal{R}$  composed a specific orthogonal block.

**Step 3:** Remove  $\mathcal{R}$  from the current vertex set  $\mathcal{E}$  and denote the set of the remaining vertices as  $\mathcal{C} = \mathcal{V}/\mathcal{R}$ . If  $\mathcal{C} = \emptyset$ , terminate the algorithm; Otherwise, return to Step 2.

Upon assuming that there are  $L$  blocks to be found, the complexity of the DFS algorithm in each iteration is on the order of  $\mathcal{O}(|\mathcal{V}|/L + |\mathcal{E}|/L)$  [21].

### C. Low-Complexity Detection

Once  $L$  orthogonal blocks have been identified, the data symbol can be detected block by block. Specifically, any ex-

isting detection algorithm can be invoked for each orthogonal block.

According to (14), since the size of the channel matrix  $\tilde{\mathbf{H}}_i, i = 1, \dots, L$  is much lower than that of the original channel matrix  $\mathbf{H} \in C^{NM \times NM}$ , the detection complexity may be significantly reduced. Furthermore, since the blocks are orthogonal to each other, there is no performance loss.

The total complexity of DFS imposed by determining these  $L$  orthogonal blocks is  $\mathcal{O}(MN(P+2))$ . Furthermore, for each orthogonal block, the size of the channel matrix for each orthogonal block is  $(MN/L \times MN/L)$ . When an MMSE detector is used, for each orthogonal block, the complexity order is  $\mathcal{O}((\frac{MN}{L})^3)$ , and the total detection complexity order of  $L$  blocks is  $\mathcal{O}(\frac{(MN)^3}{L^2})$ . Hence, the total complexity of the OB based MMSE detection scheme including the DFS and MMSE detectors is  $\mathcal{O}(MN(P+2)) + \mathcal{O}(\frac{(MN)^3}{L^2}) \approx \mathcal{O}(\frac{(MN)^3}{L^2})$ . By contrast, for the traditional MMSE detector operating without our partitioning algorithm, as the size of the whole block is  $(MN \times MN)$ , the complexity order is  $\mathcal{O}((NM)^3)$ . Hence, the complexity of our OB-based MMSE detector is approximately a fraction  $\frac{1}{L^2}$  of the traditional MMSE detector.

Furthermore, when the MP detector is used, assuming that the number of iterations for each OB is  $n_1$ , the complexity order of the MP detector is  $\mathcal{O}((n_1(NM/L)P|\mathcal{A}|))$ , and the total detection complexity order of  $L$  blocks is  $\mathcal{O}(n_1MNP|\mathcal{A}|)$ . Hence, the total complexity of our OB based MP detection scheme including the DFS and MP detection is  $\mathcal{O}(MN(P+2)) + \mathcal{O}(n_1MNP|\mathcal{A}|) \approx \mathcal{O}(NM(n_1P|\mathcal{A}| + P+2))$ . By contrast, for the traditional MP detector, assuming that the number of iterations is  $n_2$ , the complexity order is  $\mathcal{O}(n_2MNP|\mathcal{A}|)$ . As the size of each OB is much lower than the original block, the number of iterations for each OB may be less than that for the original block, i.e.  $n_1 < n_2$ . Hence, the OB based MP detection scheme still has a lower complexity than the traditional MP detection scheme. Furthermore, if the delay and Doppler spread remains unchanged, the OB block is the same for each OTFS block. Hence, the DFS algorithm is only needed for the first OTFS block and the complexity of the DFS is only counted once.

*Remark 1:* Indeed, there may exist fractional Doppler shifts in OTFS. In this case, a single data symbol may traverse more than just a few paths and affects more received signals as explained in [9]. Consequently, the orthogonal block nature would not hold any more. Hence, our orthogonal block (OB) based low-complexity optimal detection scheme would no longer be beneficial. However, channel estimation is also needed for our OTFS system. One of the popular channel estimation schemes relies on embedded pilots, where guard intervals are also required [22]. In this case, the pilot and guard intervals can be carefully designed to separate the different blocks. Hence, orthogonal blocks can be created and our OB-based scheme can be extended to the scenario of fractional Doppler shifts.

## IV. SIMULATION RESULTS

In this section, we characterize the performance of the proposed OB based detector of the OTFS system. Specifically,

the total number of subcarriers is set to  $M = 64$  and the total number of carriers is set to  $N = 32$ . Furthermore, QPSK modulation is used. Moreover, the complex Gaussian channel is assumed, which models an uncorrelated Rayleigh-fading channel.

In Fig. 2, the number of orthogonal blocks versus the number of paths is plotted, for  $P = 2, 3, 4$  and  $5$ , respectively by using the proposed orthogonal block identification algorithm. The indices of the channel delay and Doppler are listed in Table II. Observe from Fig.2 that number of orthogonal blocks is reduced upon increasing the number of paths. Specifically, the number of orthogonal blocks is  $L = 64, 8, 1$  and  $1$  for  $P = 2, 3, 4$  and  $5$ , respectively. Explicitly, when the number of paths increases, the received signal consists of more transmitted symbols, and hence a block contains more signals, which results in fewer orthogonal blocks. Furthermore, there are certain high-mobility scenarios having only a few paths in UAV communication, where typically a two-Ray channel model is assumed as the air-to-ground propagation channel model [23].

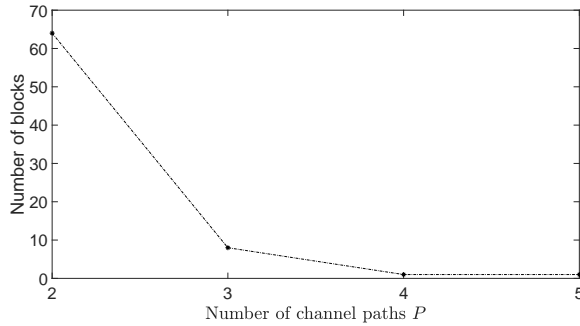


Fig. 2: The number of orthogonal blocks versus the number of paths, when the number of paths in the channel is  $P = 2, 3, 4$  and  $5$ , respectively.

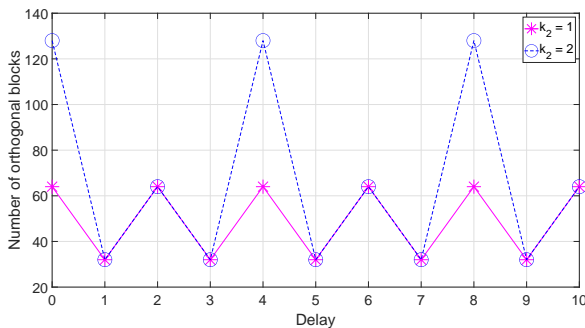


Fig. 3: The number of orthogonal blocks versus the delay of paths, when the number of paths in the channel is  $P = 2$ .

In Fig.3, the number of orthogonal blocks versus the delay of paths is plotted when the number of paths in the channel is  $P = 2$  for  $k_2 = 1$  and  $k_2 = 2$ , respectively. As we can see from Fig.3, that the number of orthogonal blocks varies for different delay.

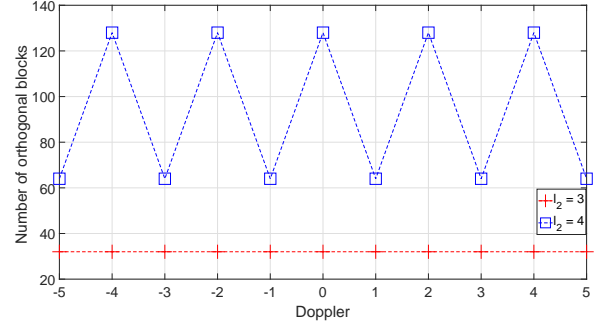


Fig. 4: The number of orthogonal blocks versus the doppler of paths, when the number of paths in the channel is  $P = 2$ .

In Fig.4, the number of orthogonal blocks versus the Doppler shift is plotted when the number of paths in the channel is  $P = 2$  for  $l_2 = 3$  and  $l_2 = 4$ , respectively. As we can see from Fig.4, that the number of orthogonal blocks varies for different Doppler shift.

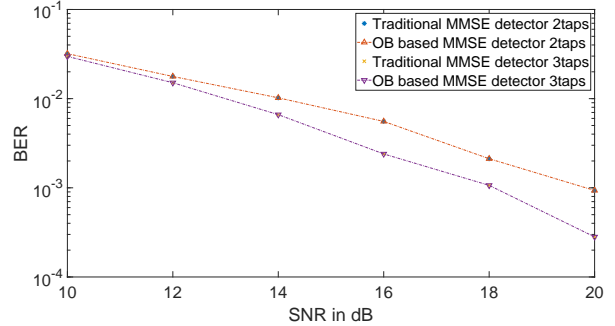


Fig. 5: The BER performance versus the SNR for both the OB based MMSE detector and the traditional MMSE OTFS detector.

In Fig. 5, the BER versus SNR performance is shown for both our OB based MMSE detector and the traditional MMSE detector for  $P = 2$  and  $3$  paths, respectively. The indices of channel delay and Doppler bins are listed in Table II for  $P = 2$  and  $P = 3$ . Consequently, the number of orthogonal blocks is  $L = 64$  and  $8$  for  $P = 2$  and  $P = 3$ , respectively. As seen from Fig. 5, the OB based MMSE detector achieves the same performance as the traditional MMSE detector. However, the complexity is only a fraction of  $\frac{1}{4096}$  and  $\frac{1}{64}$  of the traditional MMSE detector for  $P = 2$  and  $P = 3$ , respectively.

## V. CONCLUSION

In this treatise, an optimal low-complexity OB based detector was designed for OTFS systems associated with integer Doppler shifts and low-dispersion channels. This was achieved without any performance loss as a benefit of partitioning the received signals into orthogonal blocks. For each orthogonal block, any of the existing detection scheme can be used.

## VI. ACKNOWLEDGEMENT

The insightful suggestions of Dr. Chao Xu, ECS University of Southampton, provided during the revision of the paper are gratefully acknowledged.

TABLE II: Simulation Parameters

Number of paths	Indices of delay and Doppler
2	$l_1 = 0, k_1 = 0; l_2 = 2, k_2 = 1$
3	$l_1 = 0, k_1 = 0; l_2 = 2, k_2 = 1; l_3 = 4, k_3 = -2$
4	$l_1 = 0, k_1 = 0; l_2 = 2, k_2 = 1; l_3 = 4, k_3 = -2; l_4 = 5, k_4 = -4$
5	$l_1 = 0, k_1 = 0; l_2 = 2, k_2 = 1; l_3 = 4, k_3 = -2; l_4 = 5, k_4 = -4; l_5 = 6, k_5 = -2$

## REFERENCES

- [1] C. Xu, T. Bai, J. Zhang, R. Rajashekar, R. G. Maunder, Z. Wang, and L. Hanzo, "Adaptive coherent/non-coherent spatial modulation aided unmanned aircraft systems," *IEEE Wireless Communications*, vol. 26, no. 4, pp. 170–177, 2019.
- [2] J. Zhang, T. Chen, S. Zhong, J. Wang, W. Zhang, X. Zuo, R. G. Maunder, and L. Hanzo, "Aeronautical *ad hoc* networking for the internet-above-the-clouds," *Proceedings of the IEEE*, vol. 107, no. 5, pp. 868–911, 2019.
- [3] J. Shi, J. Hu, Y. Yue, X. Xue, W. Liang, and Z. Li, "Outage probability for OTFS based downlink LEO satellite communication," *IEEE Transactions on Vehicular Technology*, vol. 71, no. 3, pp. 3355–3360, 2022.
- [4] Z. Wei, W. Yuan, S. Li, J. Yuan, G. Bharatula, R. Hadani, and L. Hanzo, "Orthogonal time-frequency space modulation: A promising next-generation waveform," *IEEE Wireless Communications*, vol. 28, no. 4, pp. 136–144, 2021.
- [5] R. Hadani, S. Rakib, M. Tsatsanis, A. Monk, A. J. Goldsmith, A. F. Molisch, and R. Calderbank, "Orthogonal time frequency space modulation," in *2017 IEEE Wireless Communications and Networking Conference (WCNC)*, 2017, pp. 1–6.
- [6] R. Hadani and A. Monk, "OTFS: A new generation of modulation addressing the challenges of 5G," *arXiv e-prints*, p. arXiv:1802.02623, Feb. 2018.
- [7] C. Xu, L. Xiang, J. An, C. Dong, S. Sugiura, R. G. Maunder, L.-L. Yang, and L. Hanzo, "OTFS-aided RIS-assisted SAGIN systems outperform their OFDM counterparts in doubly-selective high-Doppler scenarios," *IEEE Internet Things J.*, pp. 1–1, 2022.
- [8] K. R. Murali and A. Chockalingam, "On OTFS modulation for high-Doppler fading channels," in *2018 Information Theory and Applications Workshop (ITA)*, 2018, pp. 1–10.
- [9] P. Raviteja, K. T. Phan, Y. Hong, and E. Viterbo, "Interference cancellation and iterative detection for orthogonal time frequency space modulation," *IEEE Transactions on Wireless Communications*, vol. 17, no. 10, pp. 6501–6515, 2018.
- [10] W. Yuan, Z. Wei, J. Yuan, and D. W. K. Ng, "A simple variational Bayes detector for orthogonal time frequency space (OTFS) modulation," *IEEE Transactions on Vehicular Technology*, vol. 69, no. 7, pp. 7976–7980, 2020.
- [11] L. Li, Y. Liang, P. Fan, and Y. Guan, "Low complexity detection algorithms for OTFS under rapidly time-varying channel," in *2019 IEEE 89th Vehicular Technology Conference (VTC2019-Spring)*, 2019, pp. 1–5.
- [12] F. Liu, Z. Yuan, Q. Guo, Z. Wang, and P. Sun, "Multi-block UAMP based detection for OTFS with rectangular waveform," *IEEE Wireless Communications Letters*, pp. 1–1, 2021.
- [13] Z. Gong, S. Liu, and Y. Huang, "Doppler diversity reception for OTFS modulation," in *Proc. IEEE 95th Veh. Techn. Conf. (VTC-Spring)*, Helsinki, Finland, 2022, pp. 1–6.
- [14] T. Thaj and E. Viterbo, "Low complexity iterative Rake decision feedback equalizer for zero-padded OTFS systems," *IEEE Transactions on Vehicular Technology*, vol. 69, no. 12, pp. 15 606–15 622, 2020.
- [15] S. Li, W. Yuan, Z. Wei, J. Yuan, B. Bai, D. W. K. Ng, and Y. Xie, "Hybrid MAP and PIC detection for OTFS modulation," *IEEE Transactions on Vehicular Technology*, vol. 70, no. 7, pp. 7193–7198, 2021.
- [16] S. Li, W. Yuan, Z. Wei, and J. Yuan, "Cross domain iterative detection for orthogonal time frequency space modulation," *IEEE Transactions on Wireless Communications*, pp. 1–1, 2021.
- [17] G. D. Surabhi and A. Chockalingam, "Low-complexity linear equalization for OTFS modulation," *IEEE Communications Letters*, vol. 24, no. 2, pp. 330–334, 2020.
- [18] Y. Fan, S. Gao, X. Cheng, L. Yang, and N. Wang, "Wideband generalized beamspace modulation (wGBM) for mmwave massive MIMO over doubly-selective channels," *IEEE Transactions on Vehicular Technology*, vol. 70, no. 7, pp. 6869–6880, 2021.
- [19] Q. Spencer, A. Swindlehurst, and M. Haardt, "Zero-forcing methods for downlink spatial multiplexing in multiuser mimo channels," *IEEE Transactions on Signal Processing*, vol. 52, no. 2, pp. 461–471, 2004.
- [20] P. Raviteja, K. T. Phan, Q. Jin, Y. Hong, and E. Viterbo, "Low-complexity iterative detection for orthogonal time frequency space modulation," in *2018 IEEE Wireless Communications and Networking Conference (WCNC)*, 2018, pp. 1–6.
- [21] T. H. Cormen, C. E. Leiserson, R. L. Rivest, C. Stein, M. London, M. B. Company, and B. B. Ridge, "Introduction to algorithms, 3rd edition," in *The MIT Press*, 1996.
- [22] P. Raviteja, K. T. Phan, and Y. Hong, "Embedded pilot-aided channel estimation for otfs in delaydoppler channels," *IEEE Transactions on Vehicular Technology*, vol. 68, no. 5, pp. 4906–4917, 2019.
- [23] W. Khawaja, I. Guvenc, D. W. Matolak, U.-C. Fiebig, and N. Schneckenburger, "A survey of air-to-ground propagation channel modeling for unmanned aerial vehicles," *IEEE Communications Surveys Tutorials*, vol. 21, no. 3, pp. 2361–2391, 2019.